CHAPTER II

CALCULATION OF ELECTROMAGNETIC FIELDS

(A) Dielectric model and Electromagnetic Field:

In this chapter, we shall discuss the calculation of the electromagnetic field in a solid when electromagnetic radiation is incident on it. This is an extremely complex problem and ab initio calculations have been done only for jellium in the presence of a surface. However, these calculations have not been extended to other metals where the jellium model is not applicable. Consequently, if one wants to consider the field variation in the presence of the surface for metals e.g., transition metals like tungsten, molybdenum, palladium, chromium etc, one has to consider simpler models. Such a model used by Bagchi, Barrera and Kar[21,22] for tungsten has been adopted for the calculation of the electromagnetic field in the surface region. Although this model involving a linear interpolation in the surface region between the experimentally determined bulk dielectric function and the vacuum value, has some shortcomings, perhaps the most important being that it is a local response function, it has the virtue of being tractable and as evidenced by the application to tungsten[21] and aluminium[23,24], it also gives reasonably good

results. Since the input required for this model is experimentally obtained[25] bulk dielectric value, the field calculation can also be extended to the case of semiconductors. In the following, we briefly describe the model and the calculation of the electromagnetic fields from it. We shall then discuss the application of this model to a number of cases.

The dielectric model used is the one given by Bagchi and Kar[21] which is shown in Fig. (2.1). The metal is assumed to occupy the space to the left of $z=0$ plane which is the nominal surface plane. In the region $-a/2 \leq z \leq a/2$, the dielectric constant is chosen to be a local function which interpolates linearly between the bulk value inside the metal and the vacuum value (unity) outside. The model frequency dependent dielectric function is:

$$\varepsilon(\omega,z) = \begin{cases} \varepsilon(\omega) = \varepsilon_1(\omega) + i\varepsilon_2(\omega), & z \leq -a/2 \\ \frac{1}{2}\left[1 + \varepsilon(\omega)\right] + \left[1 - \varepsilon(\omega)\right]\frac{z}{a}, & -a/2 \leq z \leq a/2 \\ 1, & z \geq a/2 \end{cases} \qquad (2.1)$$

The incident radiation was taken to be p - polarised of frequency ω. It was incident on the surface defined by x-y plane at an angle of incidence θ_i. A gauge was chosen in which the scalar potential is set equal to zero and the

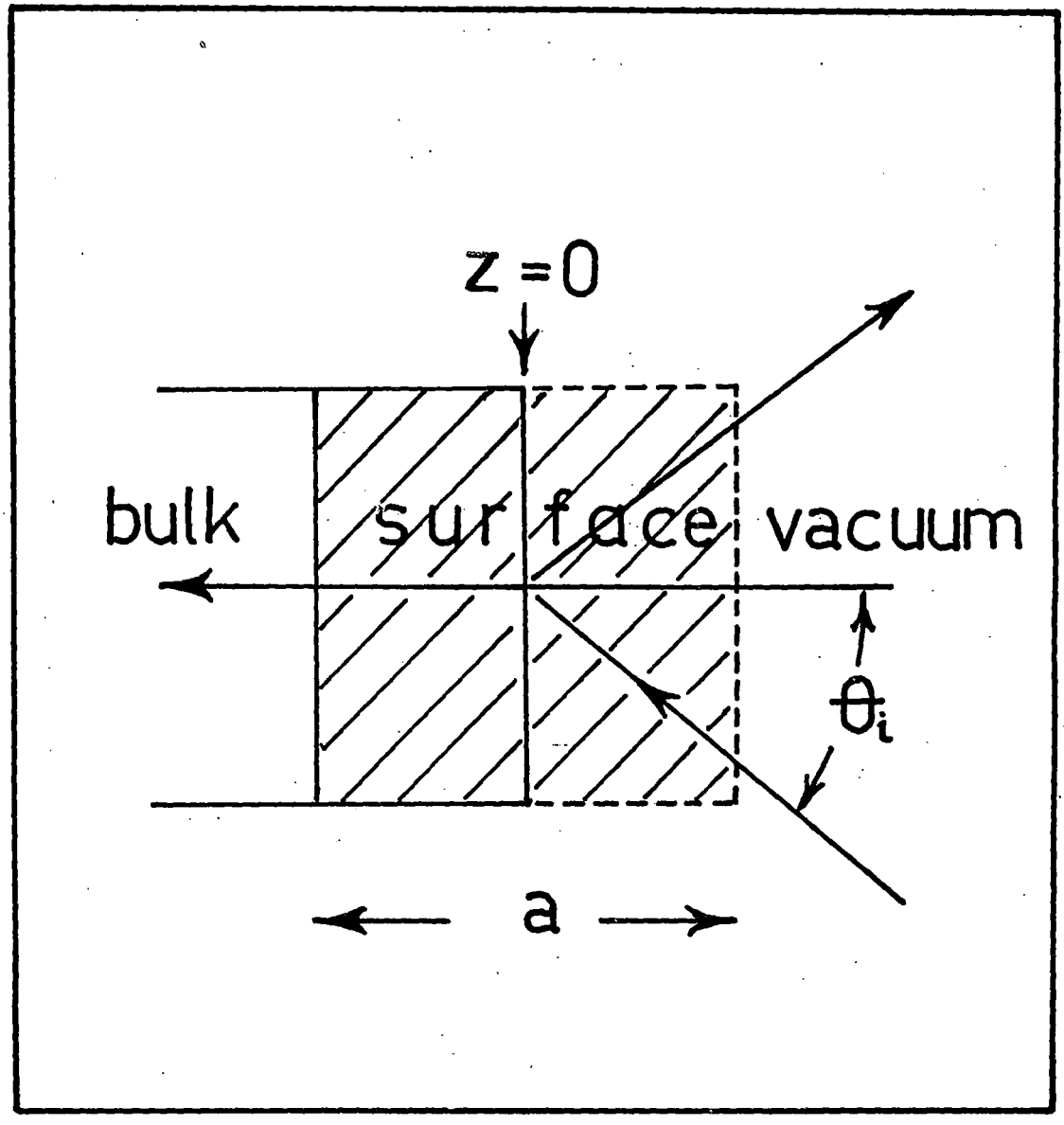

Figure 2.1

electromagnetic field $\vec{E}(\vec{Q},\omega;z)$ is expressed in terms of vector potential $\vec{A}(\vec{Q},\omega,z)$ as

$$\vec{E}(\vec{Q},\omega;z) = \frac{i\omega}{c}\vec{A}(\vec{Q},\omega;z)$$

where $Q = (\omega/c)\sin\theta_i$. The magnetic field $B(z)=B(\vec{Q},\omega;z)$ points in the y- direction and it obeys the following equation:

$$\frac{d}{dz}\left(\frac{1}{\varepsilon}\frac{dB}{dz}\right) + \left(\frac{\omega^2}{c^2} - \frac{Q^2}{\varepsilon}\right) B = 0 \qquad (2.2)$$

where $\varepsilon = \varepsilon(\omega;z)$. The electric field components can be obtained from the magnetic field as

$$E^x(\vec{Q},\omega;z) = \frac{c}{i\omega\varepsilon}\frac{dB}{dz}$$

$$E^z(\vec{Q},\omega;z) = -\frac{\sin\theta_i}{\varepsilon} B \qquad (2.3)$$

To solve Eq. (2.2), a new variable $u(z)$ was introduced according to prescription of Landau and Lifshitz which is given by $B(z) = u(z)\sqrt{\varepsilon}$. $u(z)$ then satisfies the equation

$$\frac{d^2u}{dz^2} + \frac{\omega^2}{c^2}(\varepsilon - \sin^2\theta_i)u + \left[\frac{1}{2\varepsilon}\frac{d^2\varepsilon}{dz^2} - \frac{3}{4}\frac{1}{\varepsilon^2}\left(\frac{d\varepsilon}{dz}\right)^2\right]u = 0 \qquad (2.4)$$

For the dielectric model used, $d\varepsilon/dz$ is finite only in the

region $-a/2 \leq z \leq a/2$ and $d^2\varepsilon/dz^2$ vanishes everywhere except for singularities at $z=\pm a/2$. Matching the fields at the boundary points, the magnetic and electric fields were obtained. The normal component of the electric field in the long wavelength limit as deduced by Bagchi and Kar[21] is:

$$\tilde{A}_{\omega}(z) = \frac{E^{z}_{\omega}(z)}{E_{o}} =$$

$$\begin{cases} -\dfrac{\sin 2\theta_i}{[\varepsilon(\omega) - \sin^2\theta_i]^{1/2} + \varepsilon(\omega)\cos\theta_i}, & z \leq -a/2 \\[2ex] -\dfrac{\sin 2\theta_i}{\frac{z}{a} + \frac{1}{2}\left[\frac{1+\varepsilon(\omega)}{1+\varepsilon(\omega)}\right]} \cdot \dfrac{\varepsilon(\omega)/[1-\varepsilon(\omega)]}{[\varepsilon(\omega) - \sin^2\theta_i]^{1/2} + \varepsilon(\omega)\cos\theta_i}, & -a/2 \leq z \leq a/2 \\[2ex] -\dfrac{\varepsilon(\omega)\sin 2\theta_i}{[\varepsilon(\omega) - \sin^2\theta_i]^{1/2} + \varepsilon(\omega)\cos\theta_i}, & z \geq a/2 \end{cases}$$

(2.5)

The electromagnetic fields had been calculated for photon energy below and above the plasmon energy of the metals. We take the plasmon energy to be the energy at which the real part of the dielectric constant of the solids i.e., $\varepsilon_1 \rightarrow 0$. In calculating the electromagnetic field, the value of the dielectric constant $\varepsilon(\omega)$ is unity for vacuum region. For the

bulk and the surface region, we have used the experimental data for $\varepsilon(\omega)$ as given by Weaver[25] and have calculated the frequency dependence of the magnitude of $\tilde{A}_\omega(z)$ and $|\tilde{A}_\omega(z)|^2$ for a number of cases. $|\tilde{A}_\omega(z)|^2$ was calculated as the photoemission cross-section is a quadratic function of $\tilde{A}_\omega(z)$. The solids whose dielectric functions were used are the free electron metal (aluminium), noble metal (silver) and transition metals like rhodium, molybdenum and palladium as well as silicon. $|\tilde{A}_\omega(z)|^2$ has been plotted against photon energy ($\hbar\omega$) for different planes in the surface region,i.e., for a number of values of z/a. Real and imaginary parts of $\tilde{A}_\omega(z)$ have been plotted for aluminium against z for different values of photon energy. The thickness of the surface is a parameter in our calculation. However it has been found by Appelbaum[26] that for most metals, a $\sim$ 15 Å with respect to the last plane of the atoms beyond which the electronic properties are independent of the presence of the surface and we have taken the value of a $\sim$ 10 Å.

(B) Evaluation of the electromagnetic fields:

In this section, we shall present the electromagnetic fields calculated by using the formula in Eq. (2.5) for aluminium, silver, rhodium, molybdenum, palladium and silicon. We have plotted $|\tilde{A}_\omega(z)|$ as a function of photon energy ($\hbar\omega$) and the distance (z) from the surface of the solids.

(i) Aluminium:

Fig. (2.2) shows the plot of $|\tilde{A}_\omega(z)|^2$ against the photon energy for various positions of the surface planes located at z/a=0.5 (vacuum), 0.0 (surface) and -0.5 (bulk). Here 'a' is the thickness of the surface. For regions at the surface and the bulk of the solids, we find that the graph peaks at around 11 eV and again shows a minimum at 15 eV (the plasmon energy of aluminium is taken as 15.75 eV). Also the experimental photocurrent data of Levinson et al[14] showed a peak at 11 eV and a minimum at 16 eV for the surface region of aluminium. For regions in the vacuum side, we find that in the case of aluminium, the graph shows a small peak at photon energy larger than the plasmon energy. The detailed photoemission cross-section calculation in the case of aluminium will be discussed in chapter III.

Figures (2.3) and (2.4) shows the plot of the field against distance from the surface of aluminium calculated by Thapa[27] using the dielectric function as given by jellium model:

$$\varepsilon(\omega) = 1 - \frac{\omega_p^2}{\omega^2}$$

where ω_p is the plasmon frequency of the solid. In Fig. (2.3) we show the plot of $Re\tilde{A}_\omega(z)$ and $Im\tilde{A}_\omega(z)$ for $\hbar\omega$=7.87 eV and

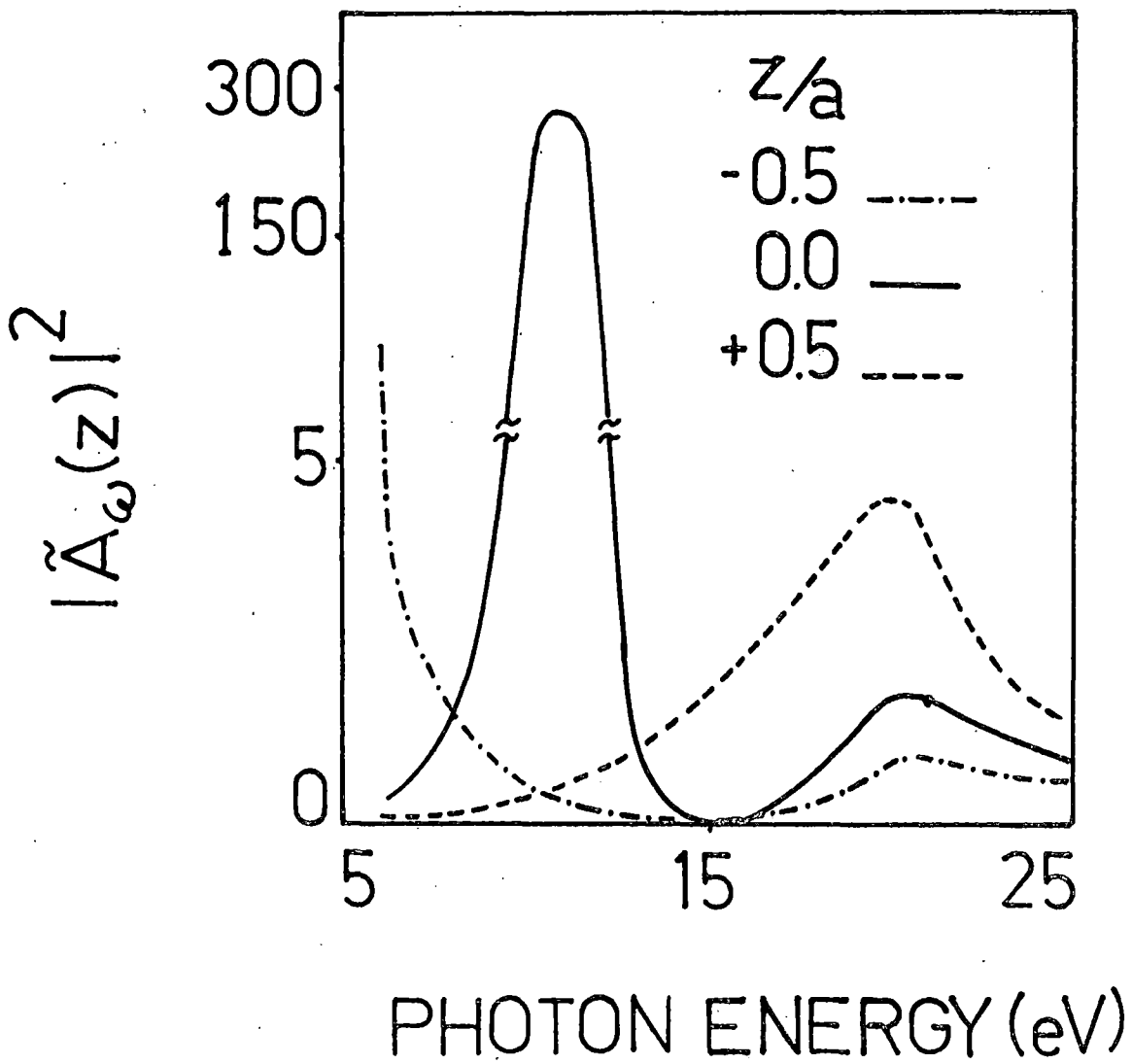

Figure 2.2

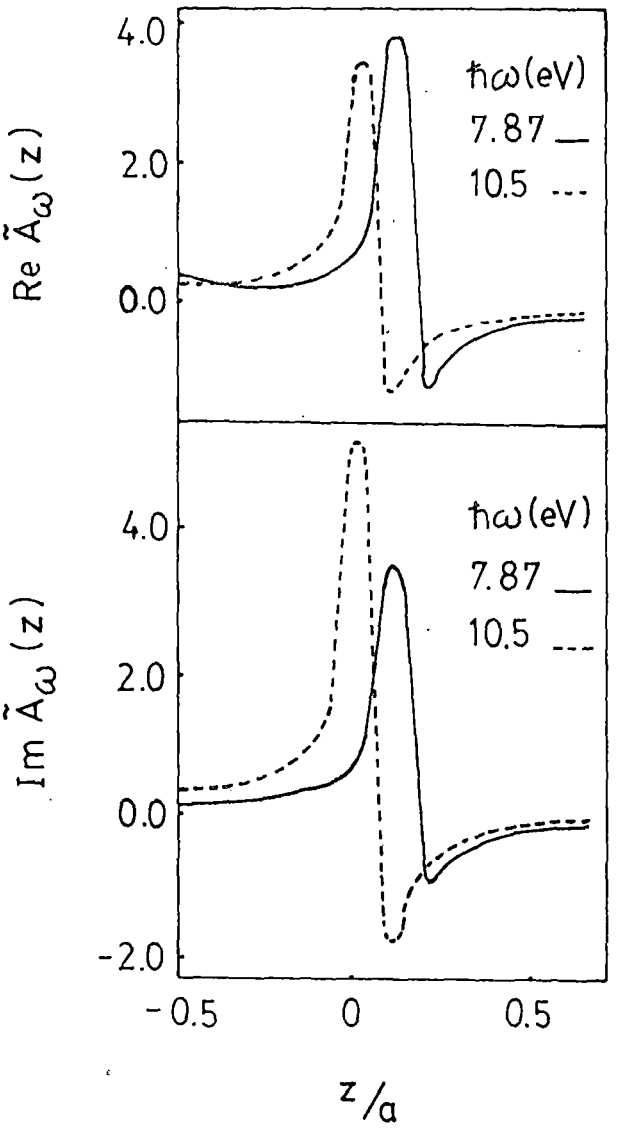
4.0
2.0
0.0
Re $\tilde{A}_\omega(z)$
$\hbar\omega$(eV)
7.87
10.5
4.0
2.0
0.0
-2.0
Im $\tilde{A}_\omega(z)$
$\hbar\omega$(eV)
7.87
10.5
-0.5
0
0.5
z/a

Figure 2.3

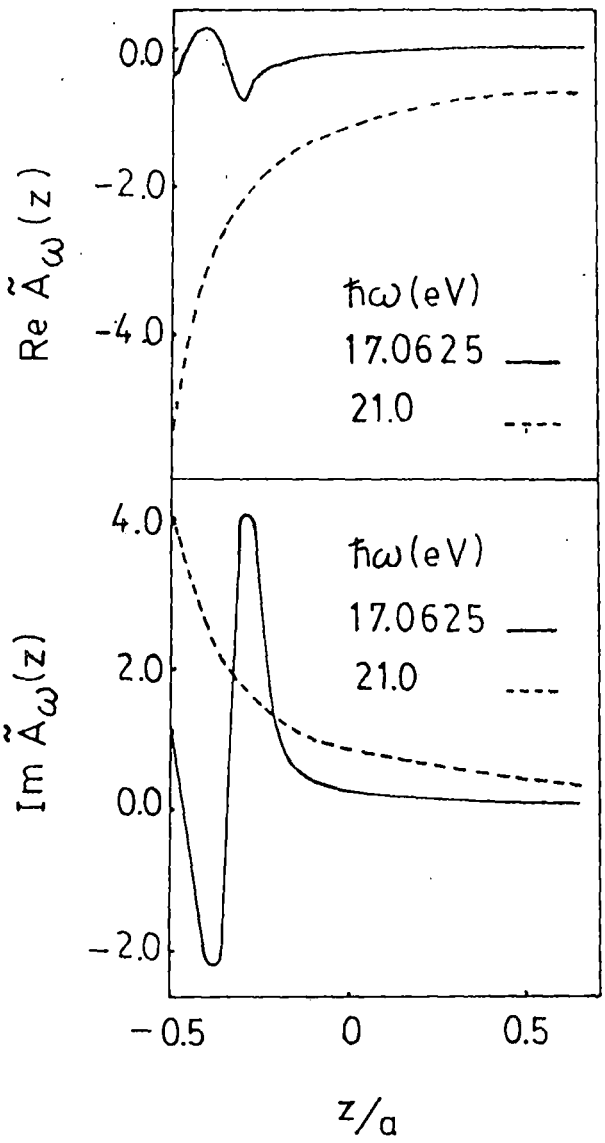
0.0
-2.0
-4.0
Re $\tilde{A}_\omega(z)$
$\hbar\omega$(eV)
17.0625
21.0
4.0
2.0
0.0
-2.0
Im $\tilde{A}_\omega(z)$
$\hbar\omega$(eV)
17.0625
21.0
-0.5
0
0.5
z/a

Figure 2.4

10.5 eV. Similarly in Fig. (2.4), the plot of $Re\tilde{A}_\omega(z)$ and $Im\tilde{A}_\omega(z)$ for photon energies at 17.065 eV and 21 eV is shown.

The behaviour of $|\tilde{A}_\omega(z)|$ as calculated by using the model of Bagchi and Kar[21] has same qualitative features like the experimental results of Levinson et al[14] but there are some differences with the data of Feibelman[13]. For example, at photon energy $\hbar\omega$ = 17.0625 eV, $Re\tilde{A}_\omega(z)$ and $Im\tilde{A}_\omega(z)$ fluctuates in the surface region in the vacuum side but decays exponentially towards the bulk region[27]. Below the plasmon energy, the real and imaginary parts of $\tilde{A}_\omega(z)$ peaks around the surface region but towards the bulk decreases exponentially. The fact that the peak is localised at the surface means that photoemission is a surface related phenomena. Moreover the magnitude of the peak height in $Im\tilde{A}_\omega(z)$ is more than that of $Re\tilde{A}_\omega(z)$ which implies that the surface phenomena is associated with the power absorption. This appears to be in agreement with the data of Feibelman[13] with the only difference that Friedel type oscillations is not exhibited towards the bulk region. This may be attributed to the locality assumption of the dielectric function in the model of Bagchi and Kar[21].

(ii) Silver:

In Fig. (2.5), we show the plot of variation of $|\tilde{A}_\omega(z)|^2$ against the photon energy for the values of z= -a/2, 0.0, and

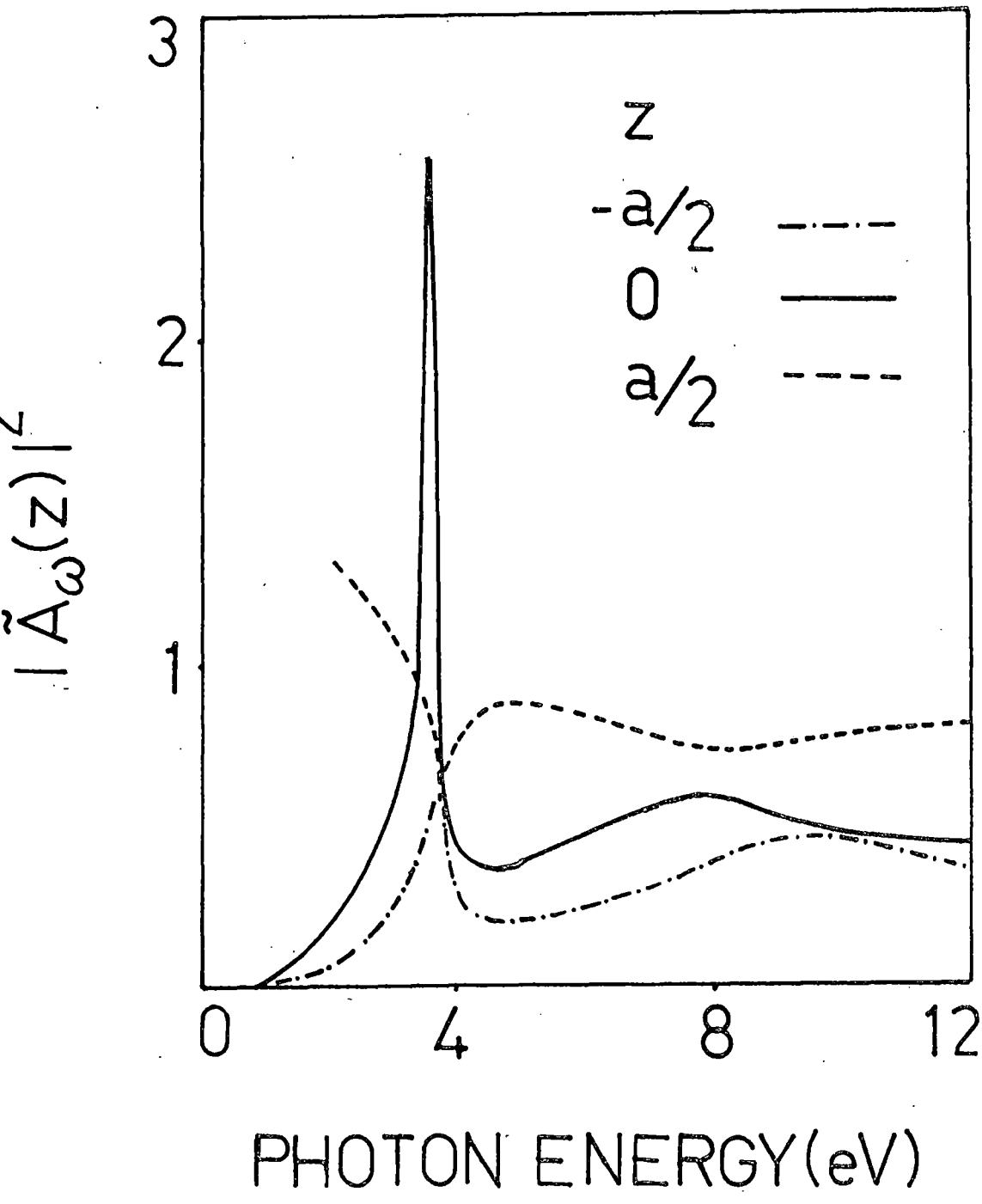

Figure 2.5

+a/2. We note that there is a sharp peak in the curve corresponding to z= 0.0 at 3.6 eV followed by a minimum at 3.9 eV which is due to surface effect. This can be concluded from the plot of $|\tilde{A}_\omega(z)|$ as a function of z for $\hbar\omega$=3.6 eV (Fig. 2.6). The peak in $|\tilde{A}_\omega(z)|$ is much weaker as we move away from 3.6 eV and at 4 eV for example, there is no peak in the surface region. Since we are using the experimentally measured dielectric function as input in our calculations, it is not possible to attribute any physical fact related to this peak. However from experimental photoemission data of Berguland and Spicer[29], it had been found that the photoemission yield is minimum at $\hbar\omega$=3.9 eV. He argued further that such phenomena is attributed to the fact that the incident photon energy near the plasmon energy have been absorbed in exciting the plasma oscillations thus not directly producing the photoelectrons.

(iii) Rhodium:

In Fig. (2.7), we are showing the plot of $|\tilde{A}_\omega(z)|^2$ as a function of the photon energy for three locations of the surface planes at z= a/2(surface), 0.0(middle of the surface) and -a/2 (bulk). The curve for z= 0.0 shows a peak at 8 eV and then has a minimum at 14 eV but increases[28] subsequently above 14 eV. If we look at $|\tilde{A}_\omega(z)|$ as a function of z for $\hbar\omega$ = 8 eV (Fig. 2.8), we see that there is a peak at z=+0.27a while for $\hbar\omega$ =14 eV, there is no peak in the surface region. So we may

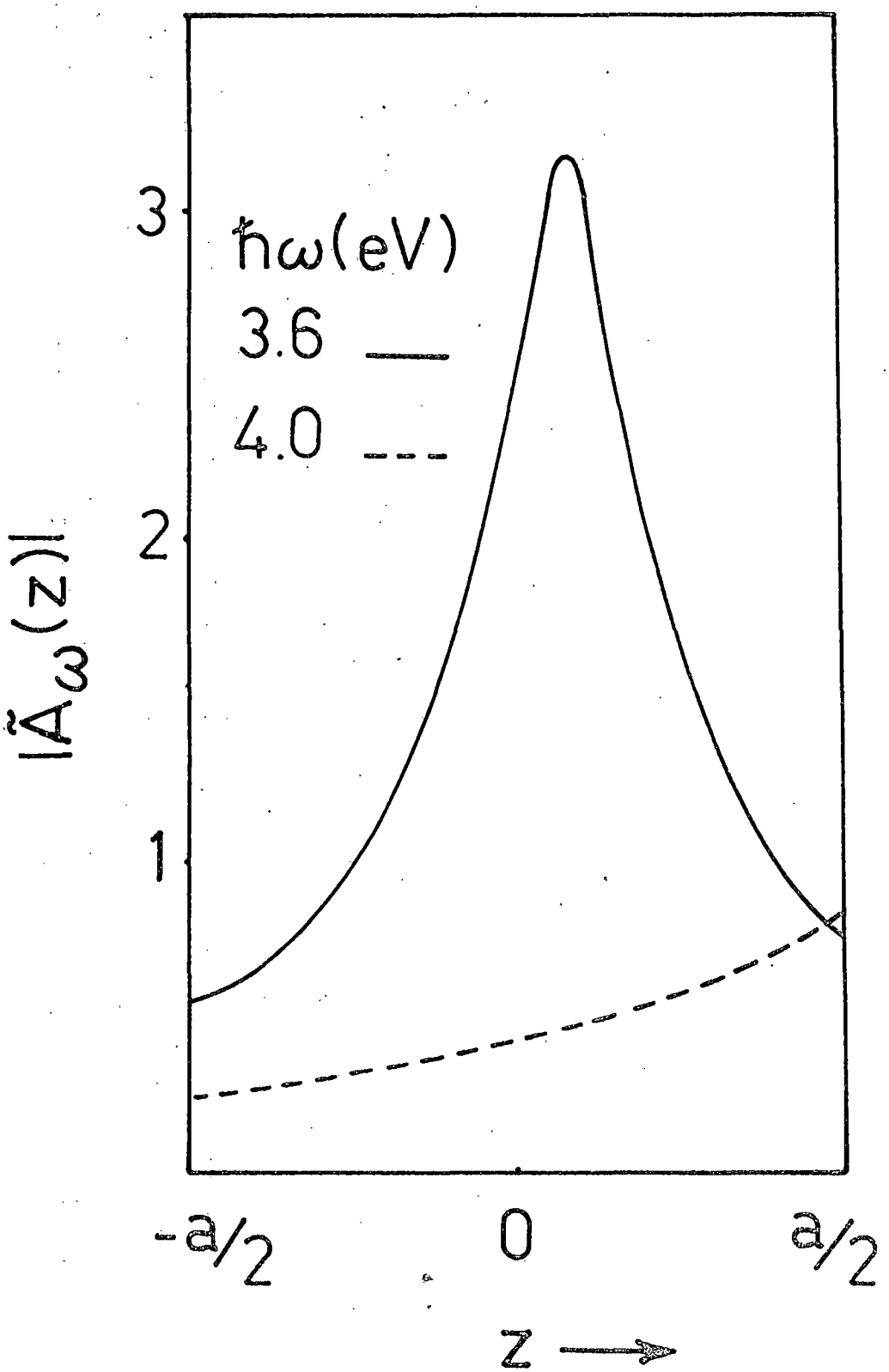

Figure 2.6

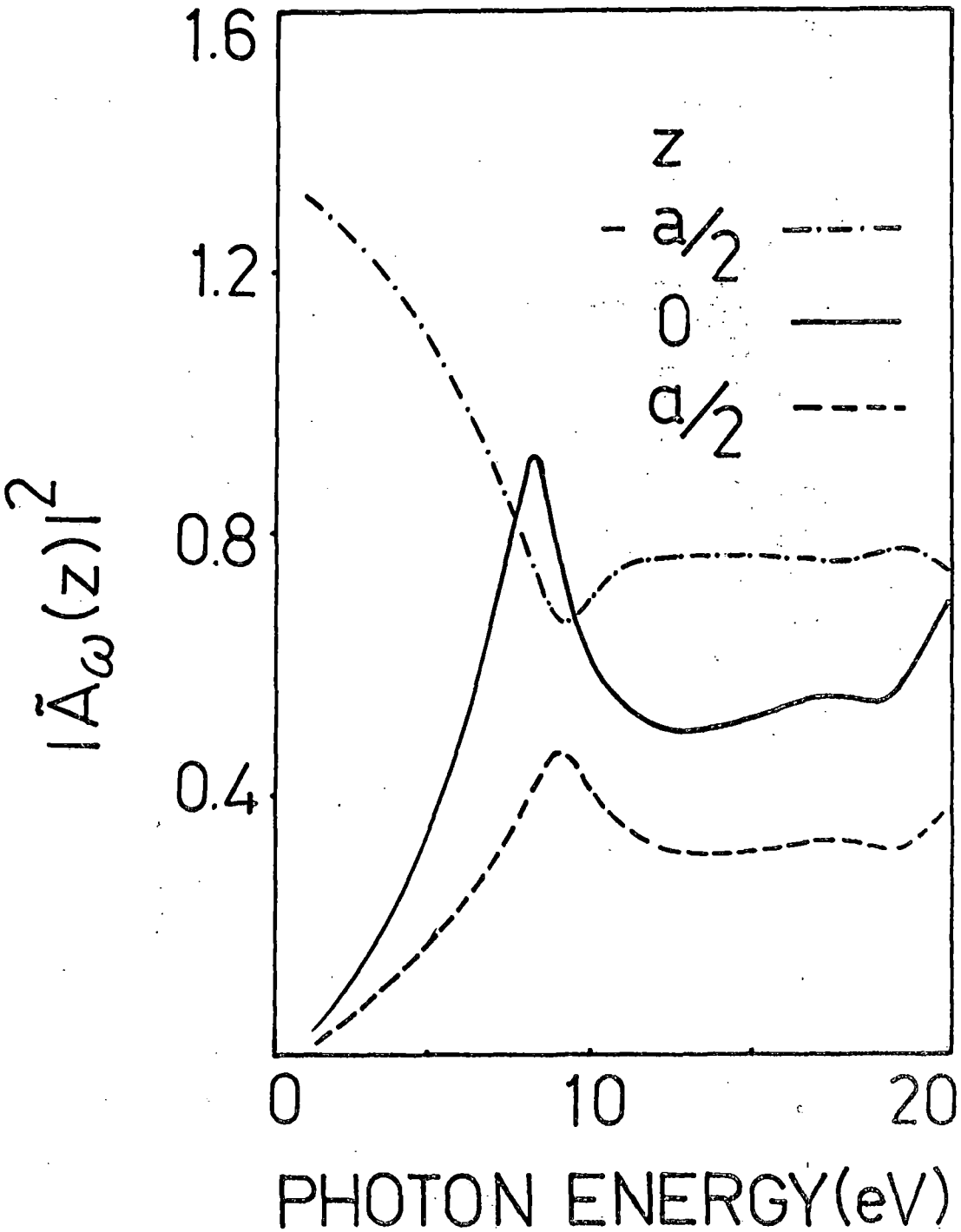

Figure 2.7

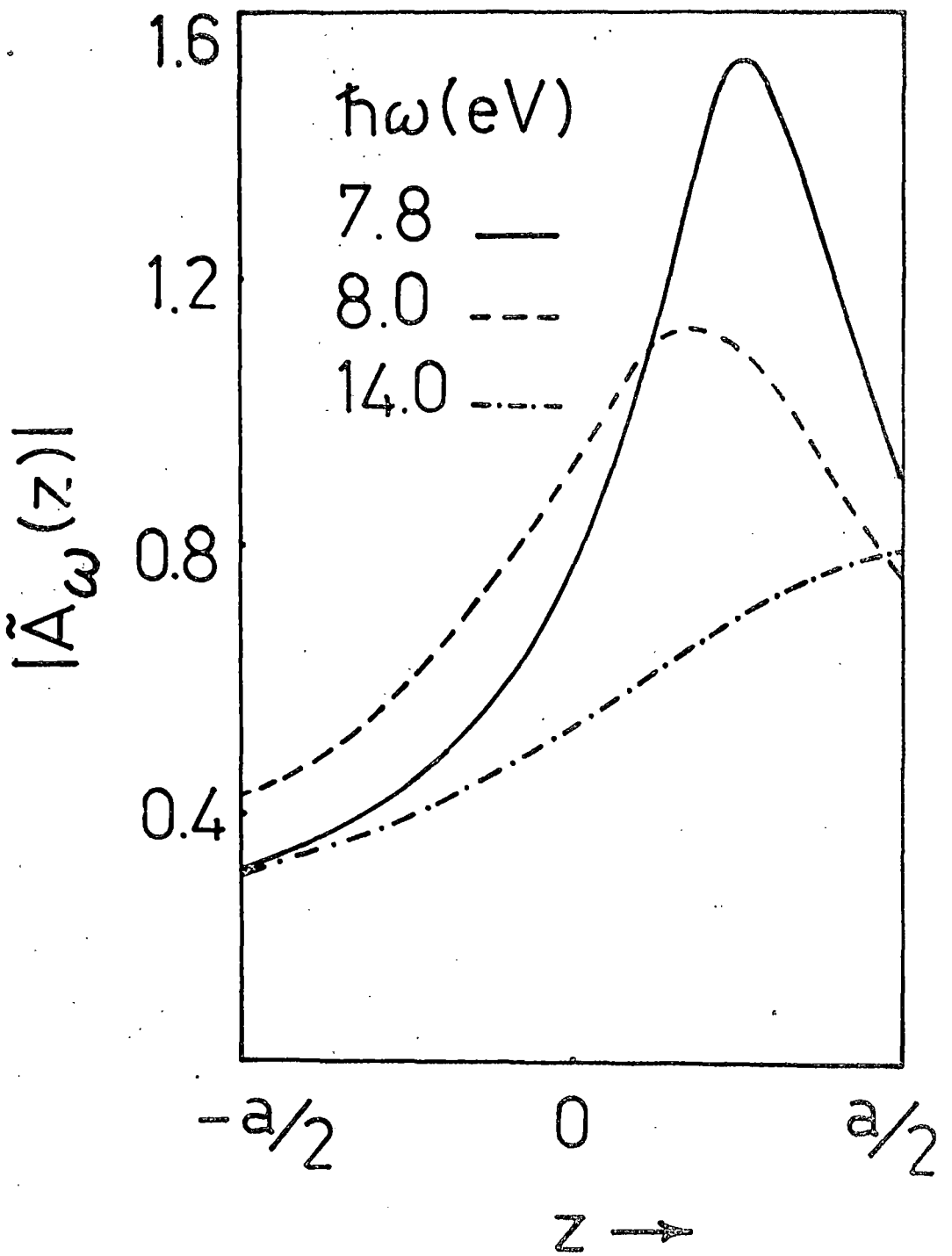

Figure 2.8

conclude that if we look at the normal photoemission there would be a peak[28] at around 8 eV which has its origin in the variation of the field in the surface region.

(iv) Molybdenum:

Fig. (2.9) shows the variation of $|\tilde{A}_\omega(z)|^2$ against photon energy for three locations of the planes at z= a/2 (vacuum - surface region interface), 0 (middle of the surface region) and -a/2 (bulk - surface region interface). The figure has a lot of structures[28] in the curves. The plot for z=0.0 shows two prominent peaks at photon energies 9.2 eV and 20 eV. Fig. (2.10) shows the plot of $|\tilde{A}_\omega(z)|$ as a function of z for photon energies 9 eV, 9.2 eV and 9.6 eV. We found that for each of these energies, there is a peak in the surface region. Also there is a peak in the surface region for energies at 19.6 eV, 20 eV and 20.6 eV as shown in (Fig.2.11). But in contrast there is no peak at 25 eV in the surface region. The photon energy dependence of $|\tilde{A}_\omega(z)|$ and $|\tilde{A}_\omega(z)|^2$ on both the sides of the interface (z=a/2 and -a/2) is quite revealing. Our calculated data of molybdenum showed qualitative features with the experimental data of Weng et al[30] who had also calculated the photon energy dependence of the field. They found that the field just outside the surface has a minimum near 25 eV and inside the surface it has a maximum at around 27 eV. For photon energy greater than 27 eV, it decreases rapidly (slowly)

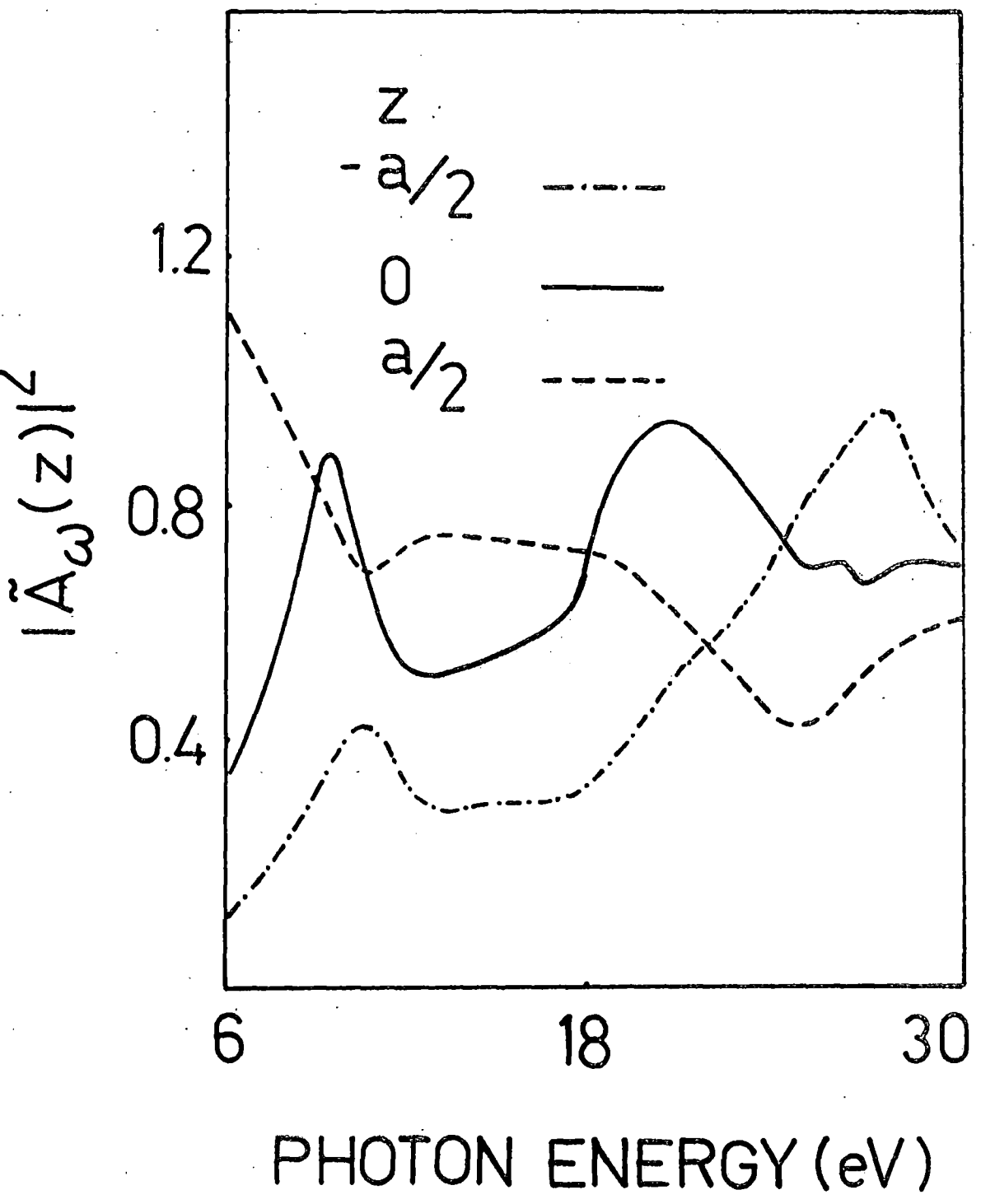

Figure 2.9

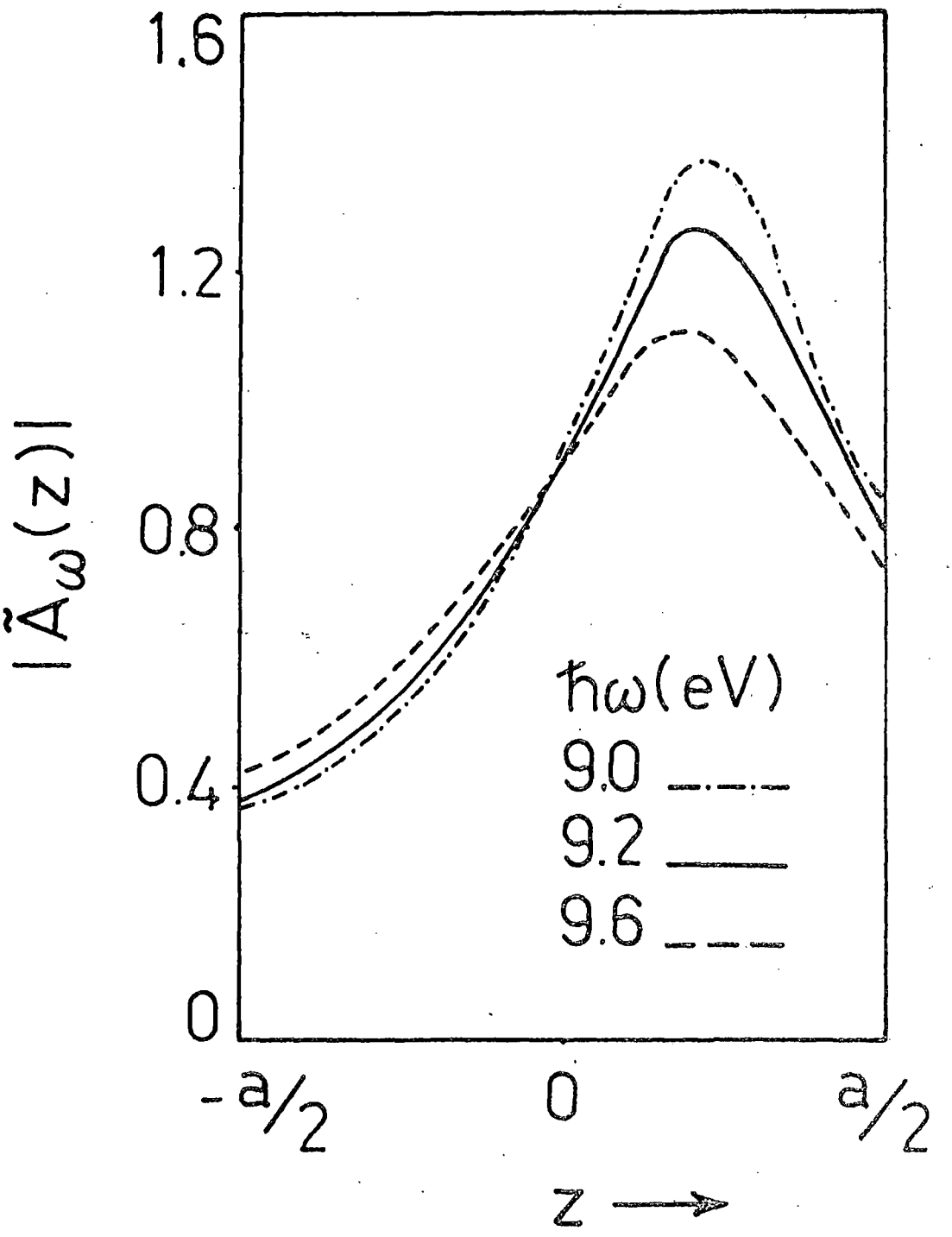

Figure 2.10

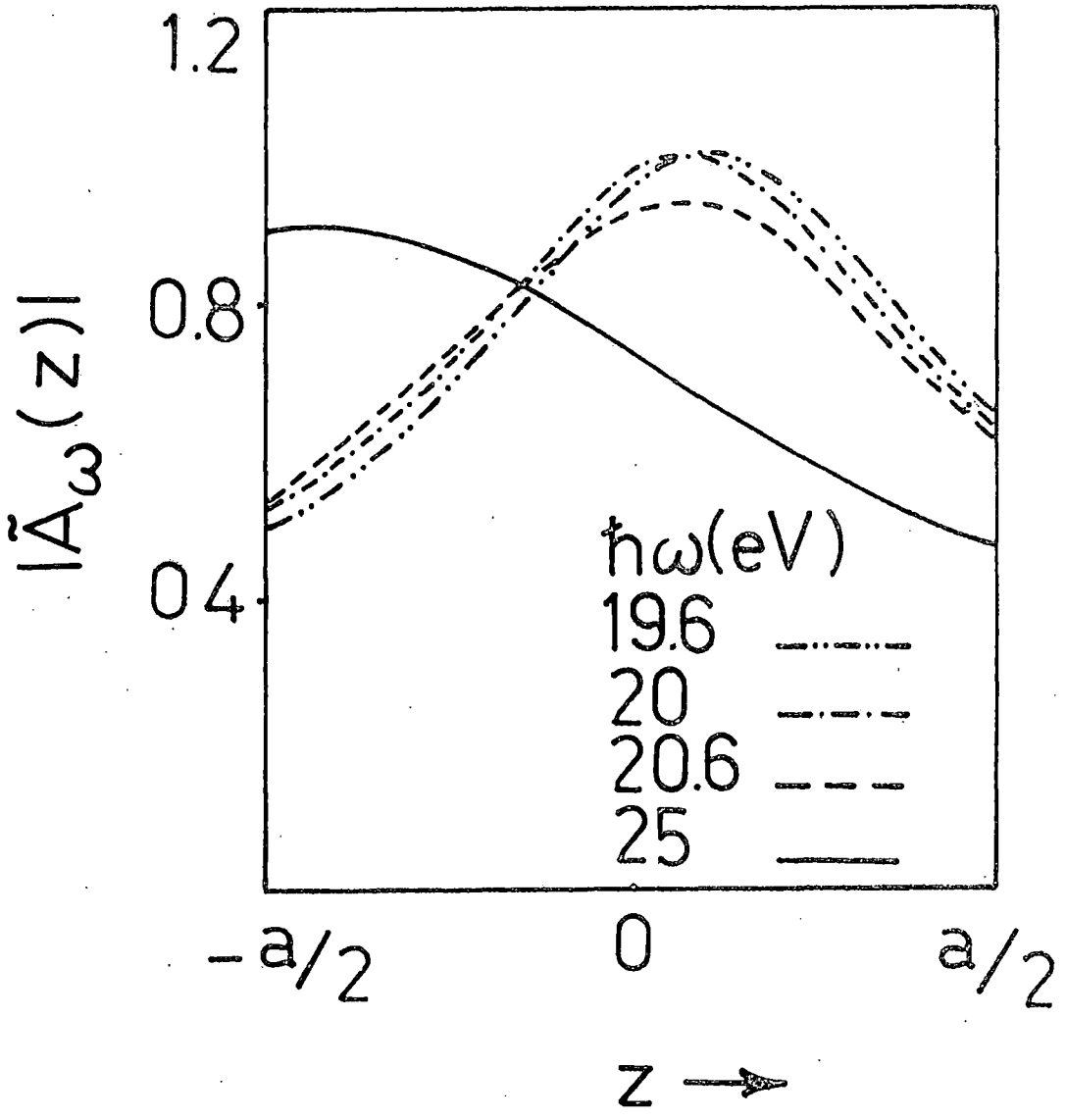

Figure 2.11

towards the low (high) photon energy side. Similar feature had been exhibited by our calculated data of field in molybdenum for region within and outside the surface (Fig. 2.9). It is found that there are two peaks at 9.5 eV and 20 eV for z = 0.0. This may be correlated to the two peaks observed in the photoemission calculation of high lying resonance for molybdenum as obtained by Weng et al[30].

(v) Palladium:

The plots of $|\tilde{A}_{\omega}(z)|^2$ against the photon energy for three location of the parallel planes at z= a/2(vacuum - surface region interface), 0.0(middle of the surface region) and -a/2(bulk - surface region interface) in case of palladium is shown in Fig. (2.12). It is found that the graph shows a minimum at photon energy 12 eV and has a peak at 7 eV. The field calculation for palladium had been reported by the author elsewhere[31]. The photon energy at 12 eV corresponds to the plasmon energy of palladium at which $\varepsilon_1 \to 0$. The calculated data of field in palladium also showed features as exhibited by other metals like aluminium, tungsten, silver etc. There is a peak in the curve at photon energy less than the plasmon energy whereas another peak smaller in height was found for photon energy greater than plasmon energy.

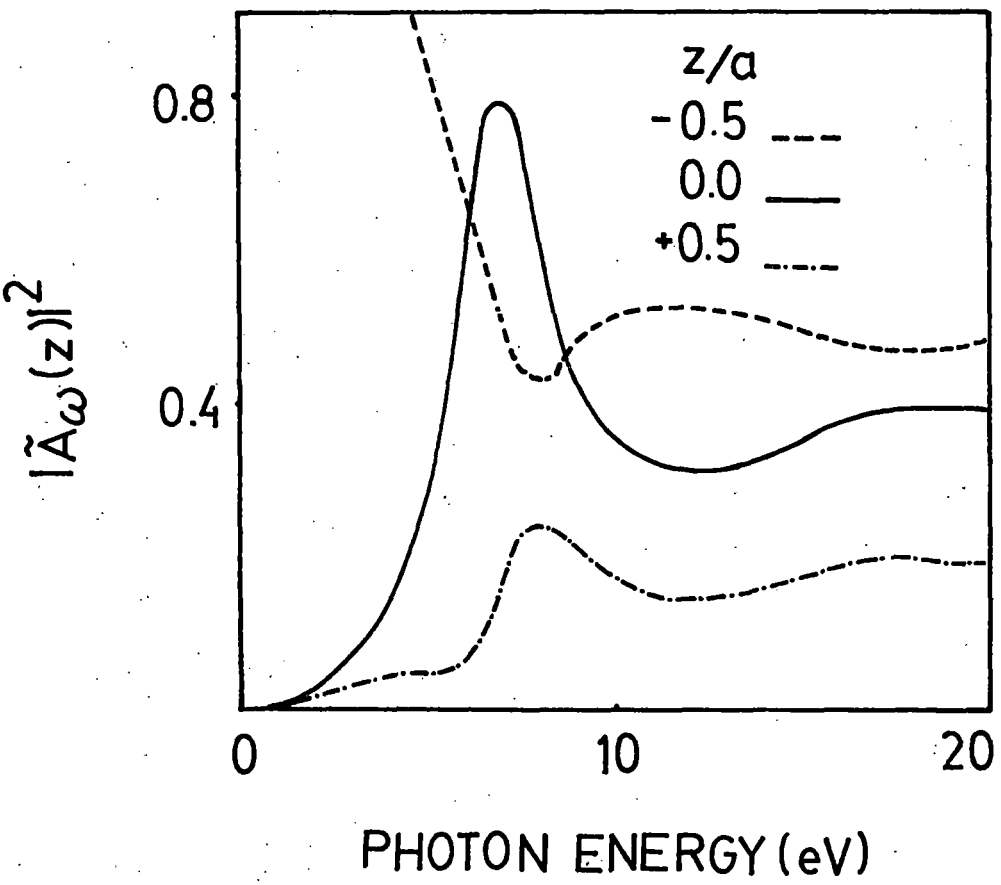

Figure 2.12

(vi) Silicon:

The presence of the surface states on the semiconductor surfaces was verified earlier by using the technique of angle integrated photoemission[32,33]. Moreover, the existence of the surface states was evident through the pinning of the Fermi level at the surface. In bulk semiconductors, the Fermi level shifts depending upon the doping level from the top of the valence band to the bottom of the conduction band. In contrast early angle integrated photoemission and work function measurements[34,35] showed that the Fermi level is pinned at the surface, almost independent of the doping level. Even though the existence of surface states on semiconductors was confirmed relatively early[36], little is known about these states compared to the surface states on metals.

Most semiconductor surfaces reconstruct. The best known example is that of Si(111) surface. A freshly cleaved surface structure can be prepared by the rapid quenching from a high temperature which stabilises the surface[37]. The Si(111) surface is only example of a variety of reconstructed semiconductor surfaces. Models for these have been developed mostly on the basis of dynamical LEED calculations. They clearly show the fundamental difference between a metal and semiconductor surfaces. For metals, reconstruction is the exception. The general behaviour is a few percent contraction of the surface

planes. In contrast semiconductors with their covalent bonding always exhibit reconstructed surfaces. The determination of the structure of semiconductor surfaces by calculating the position of surface states as a function of the structure and comparing to data has been the main objective of the angle resolved photoemission studies. Surface states on photoemission are in general s-p like unlike the case of metals, this does not imply that they are delocalised. Calculations shows that semiconductor surfaces are rather localised within certain bonds. Examples are the dangling bond structure surface states.

Since field calculations with respect to parameters like photon energy gives us the first hand informations about the photoemission cross-section, we have therefore calculated $|\tilde{A}_{\omega}(z)|^2$ against the photon energy also in the case of silicon. The plot of field square calculated against photon energy is shown in Fig. (2.13) for three different planes located at z/a=0.5(vacuum), 0.0(surface) and -0.5(bulk). We find that at the surface, there is a strong peak at 12 eV followed by a minimum at the plasmon energy 16 eV. The field then increases again but at 21 eV, it becomes very small. We note that this is the region where the dielectric function for silicon shows a resonance, as can be seen from the plots of real and imaginary parts of the dielectric function $\varepsilon(\omega)$ versus $\hbar\omega$ in Fig. (4.8). This behaviour is also reflected in the field data for the

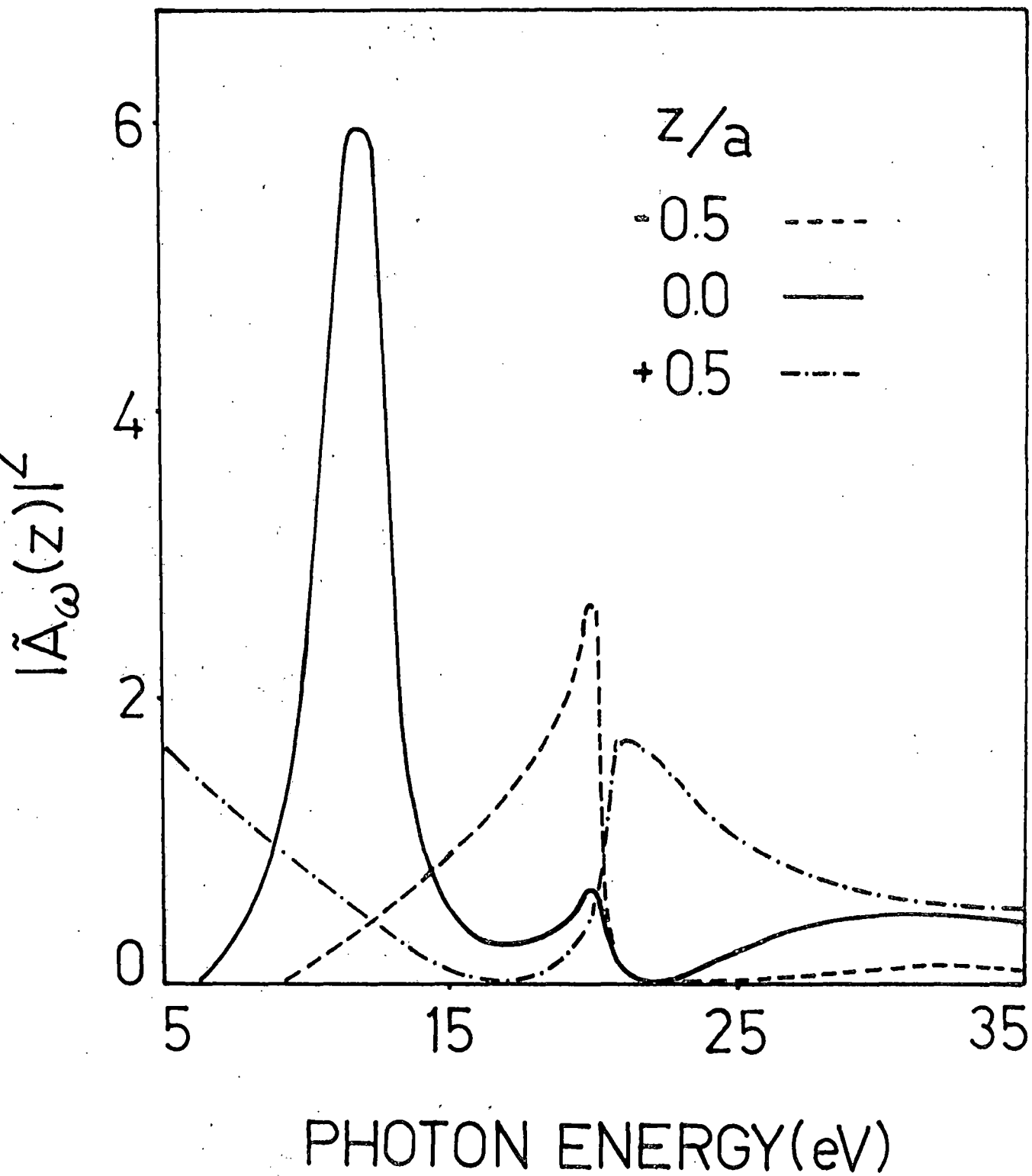

Figure 2.13

bulk-surface boundary (z/a=-0.5) which again becomes very small around 21 eV, although it does not show any minimum at the plasmon energy. The field on the vacuum-surface boundary (z/a=0.5) on the other hand shows a maximum at 21 eV and a minimum at the plasmon energy 16 eV - in direct contrast to the behaviour of the field in the bulk-surface boundary plane. This obviously points out that the variation of field in the surface region of a semiconductor is going to be quite important in photoemission calculations.